Indian Journal of Experimental Biology
Vol. 56, May 2018, pp. 293-304

Estrogenized mouse model of polycystic ovary highlights mitochondrial pathway of apoptosis

Gayatri Shinde[1], Sushma Khavale[1], Roshan Dadachanji[1], Serena D'Souza[2], Tarala Nandedkar[3] & Srabani Mukherjee[1]*

[1]Department of Molecular Endocrinology, ICMR-National Institute for Research in Reproductive Health, JM Street, Parel, Mumbai-400 012, Maharashtra, India

[2]Department of Virology, ICMR-National AIDS Research Institute, 73, 'G'-Block MIDC Bhosari, Pune-411 026, Maharashtra, India

[3]Haffkine Institute for Training, Research and Testing, Acharya Donde Marg, Parel, Mumbai-400 012, Maharashtra, India

Received 25 August 2016; *revised 28 August 2017*

Polycystic ovary syndrome, which is a major cause of anovulatory infertility in women, featured by an ovarian morphology that reflects arrested follicular growth and accumulation of cystic follicles. Alteration of apoptotic process may promote development and persistence of follicular cysts, which has not been explored in details. Female animals exposed to estrogenic compounds at specific growth stages show altered pubertal maturation, ovulatory dysfunction, accumulation of follicular cysts and infertility. Here, we developed a mouse model of cystic ovary by neonatal estrogenization and investigated apoptotic changes underlying cystogenesis across various time points. We compared pro- and anti-apoptotic markers along with ovarian morphology between control and estradiol treated mice using several techniques including flow cytometry, immunohistochemistry and electron microscopy. Treated mice presented with cystic follicles with degenerated oocyte and reduced granulosa cell layer, anovulation, along with persistent estrus cycle and infertility. Increased apoptosis was demonstrated in cystic follicles with significantly increased expression of JC-1, Bid, caspase-9 and caspase-3. Thus, our findings highlight the involvement of mitochondrial pathway of apoptosis in development of polycystic ovary in response to neonatal exposure to estrogen. This model may serve to delineate the effect of environmental estrogen exposure to altered ovarian physiology which is frequently observed in PCOS women.

Keywords: Cystic follicles, Estrogen, Infertility, Neonatal estrogenization, Polycystic ovary syndrome (PCOS)

Polycystic ovary syndrome (PCOS) is a common endocrinopathy affecting 6-10% of women of reproductive age. It is a major cause of anovulatory infertility and is commonly characterized by irregular menses, hyperandrogenemia, insulin resistance and polycystic ovaries on ultrasound[1,2]. Women with PCOS typically show ovulatory dysfunction characterized by the presence of enlarged ovaries with follicles arrested in the antral stage with accumulation of multiple cystic follicles in the periphery of the ovary i.e polycystic ovarian morphology (PCOM)[3]. During folliculogenesis many follicles undergo development and only one dominant follicle matures to form the Graafian follicle which ovulates, while other follicles undergo atresia[4-6] by the process of apoptosis[7-9]. Apoptosis is a highly complex and sophisticated process, involving an energy dependent cascade of molecular events[10] and regulates the fate of follicles during folliculogenesis[7]. In ovaries showing PCOM, the growth of follicles is arrested forming persistent cystic follicles which may be due to alteration in the apoptotic process. However, it is not possible to study the apoptotic process during the development of follicular cysts in details in the human ovary. Therefore, several groups have developed animal models of PCOS to investigate apoptotic mechanisms. A study showed a weak proliferative activity as well as a low apoptotic frequency in bovine cystic follicles[11], indicating that a static condition is maintained. Cystic follicles developed by neonatal androgenisation of rats showed increased number of apoptotic granulosa cells[12] and increased expression of Fas, FasL, and caspase 8[13]. The altered balance between pro- and antiapoptotic molecules may be intimately involved in the process of cystogenesis, and it has not been studied in detail.

Evidence indicates genetic and environmental factors may contribute to PCOS pathophysiology[14]. Exposure of endocrine disrupting compounds (EDCs) which mimic estrogen action, have been reported to

*Correspondence:
Phone: +91 22 24192009
E-mail: srabanimuk@yahoo.com; mukherjees@nirrh.res.in

exert toxic effect on female reproductive system, especially on the ovary. Administration of steroids during period of early reproductive development results in long term consequences during adult life, defined as "programming"[15]. Experimental evidences indicate that exposure to some estrogenic compounds is associated with development of polycystic ovary. Prenatal and neonatal exposure to multiple doses of estrogen leads to suppression of gonadotropins secretion, arrest of follicular development, anovulation, increased number of atretic, preantral and antral follicles, lack of ovulation, and development of follicular cysts in female rats[15-19] and mice[17]. Bisphenol A, a common EDC present in plastics is shown to reduce fertility, modify sex hormone levels and result in formation of ovarian cysts in a rodent model[20]. Thus, it can be postulated that exposure to estrogen or estrogenic EDCs may contribute to aberrant folliculogenesis along with cystic follicle development leading to PCOM which is frequently seen in women with PCOS. However, the impact of environmental estrogens on the pathogenesis of cystic follicle formation in PCOS is yet to be explored.

In the present study, we have developed a mouse model with ovarian cysts by neonatal estrogenization. The adverse effects on ovarian follicular development have been investigated along with apoptotic changes during the development of cystic follicles. We have studied ovarian histology and ultrastructure along with expression of selected pro- and antiapoptotic molecules at different time points, which is otherwise not possible to study in humans. The contribution of apoptosis in the development of cystic ovarian follicles, commonly seen in women with PCOS, may be extrapolated from this systemic study.

Materials and Methods

Experimental design

Swiss mice used in this study were bred and maintained in the experimental animal facility at the ICMR-National Institute for Research in Reproductive Health maintained on a 14 h light:10 h darkness cycle under conditions of 50% humidity and 20°C temperature, and were supplied with food and water ad libitum. Institutional Animal Ethics Committee (IAEC) approval was obtained and experiments were carried out in accordance with the guidelines for the care and use of laboratory animals specified by the Committee for the Purpose of the Supervision of Experiments on Animals (CPCSEA), India. Care was taken to ensure minimum animal suffering during sacrifice.

Treatment of animals

Six to eight week old female Swiss mice (wt. 30-32 g) were bred in the experimental animal facility and pups were kept with their biological lactating mother until weaning (21 days of age). Neonatal estrogenization of female pups in the first week post birth was carried out using previously published protocol with modification[18]. A single subcutaneous injection of 60 µg of 17β-estradiol (dissolved in 20 µL of olive oil: ethanol [9:1 v:v]) was administered at postnatal day 5. Control group consisted of vehicle treated mice which were injected with 20 µL olive oil. After this treatment, animals were sacrificed at 4, 8, 12, 16, and 20 weeks of age and ovaries were collected for assessment of various parameters. All animals were monitored each day for body weight and estrus cyclicity by examining vaginal smears each morning, after onset of puberty until sacrifice[21].

Fecundity of neonatally estrogenized mice

Control and neonatally estrogenized adult females (2 months of age) were co-housed with fertile males (2:1) for three months. Once vaginal plug was formed, animals from both groups were housed separately and monitored for pregnancy. The outcome was measured as the number of pups per female.

Ovarian histology

For each time point, ovaries from control mice were dissected during diestrus to proestrus stage. Since treated animals remained arrested in estrous phase, their ovaries were collected at the aforesaid time points. Both ovaries were carefully dissected and immersed in Bouin's fixative overnight and then transferred into 70% alcohol. After a further wash in 70% alcohol, ovaries were embedded in paraffin blocks and sectioned (5 µm) on a microtome (Leica RM2255, Wetzlar, Germany) followed by mounting on slides coated with 0.1% Poly-L-lysine (Sigma, MO, USA). The sections were stained with hematoxylin and eosin. To stain sections with hematoxylin and eosin, sections were deparaffinised by washing with xylene and rehydrated in decreasing concentrations of alcohol (100, 70, 50 and 30% each for 5 min) and water. After washing with water, sections were stained with haematoxylin for 6 min, washed with water and counter stained with eosin for 6 s and dehydrated in increasing concentration of

alcohol (70, 80, 90 and 100% for 5 s each) and section were cleared by xylene.

Atretic follicles were defined as those follicles with degenerated oocyte separated from the granulosa cells, having more than 5% of cells with pyknotic nuclei and showing fibrosis. Follicles with abnormal morphology like absence of oocyte, reduced granulosa cell layer, and thickened theca cell layer with large fluid filled antral cavity were considered as cystic follicles[16]. Double-blind morphometric analysis was conducted on every fifth section of the ovary to avoid repeated counting of the same follicle and follicle count was taken and normalized to the total area per sq mm[22].

Gonadotropin measurement

At the point of sacrifice, retro-orbital blood samples were collected at 12th week from control and treated animals and serum was stored at -20°C until further use. LH and FSH levels were measured from serum samples, diluted 1:3 with serum matrix, on Luminex 200IS platform using magnetic bead panel kits (Milliplex MAP Kits, Millipore Corporation, MA, USA) in accordance with manufacturer's instructions in duplicate.

Study of apoptosis

Ovaries were collected on ice in Dulbecco's Modified Eagle medium (DMEM) with L-glutamine (Life Technologies, NY, USA). Follicles of the entire ovary were needle punctured under the stereo-microscope (Olympus, Hamburg, Germany) to release granulosa cells into the medium. This medium was centrifuged at 1000 rpm, and the resultant cell pellet was resuspended in 1 mL medium. Three different sets of animals, each set consisting of three animals, were taken for control and treated group. Granulosa cells were pooled from ovaries of each set for both groups. Cells were counted by trypan blue exclusion test on a hemocytometer. Aliquots at a cell density of 1×10^6 cells/mL were used for analysis of viability, cell cycle and apoptotic markers (Fas, FasL and caspase 3), and mitochondrial membrane potential (MMP). All data acquisition and analysis was performed (in triplicate) on FACS Vantage SE with Argon laser (Becton Dickinson, CA, USA). Data analysis was done using Cell Quest Pro 3.1 software (BD Biosciences, CA, USA).

Viability of Granulosa cells

Cell viability, a measure of the metabolic status of a cell population was assessed by incubating cells with 1 µL fluorescent diacetate (FDA) (10 mg/mL in DMSO) (Molecular Probes, OR, USA) at 37°C for 15 min in dark. Following acquisition at 530 nm, they were expressed as number of viable cells present in the treated as compared to control group.

Cell cycle analysis

Granulosa cells were permeabilized with 0.1% NP40 diluted in phosphate buffered saline, pH 7.4 (PBS) and stained with 10 µL propidium iodide (PI) 50 µg /mL; and 8 µL DNase free RNase 40 µg/mL (Molecular Probes, OR, USA) for 15 min and acquired at 580 nm in flow cytometer. Sub G_0 cell population was compared between treated and control group as an indicator of apoptosis.

Expression of Fas/FasL and active caspase 3

One million cells were incubated with anti-Fas FITC (BD Pharmingen, USA) and FasL PE antibody (BD Pharmingen, USA) (0.5 mg/mL) at room temperature (RT) for 30 min at dark. The incubated cells were washed in fresh medium and fluorescence was detected using single filter to identify the cell population expressing the apoptotic marker Fas/FasL. Granulosa cells were stained with active caspase 3 staining kit (FITC) according to manufacturer's instructions (BD Pharmingen, USA). Cells were acquired at 530 nm and analyzed separately on FITC (for Fas and caspase 3) and PE channels for Fas L.

Detection of mitochondrial membrane potential (ψm)

JC-1(5,5',6,6'-tetrachloro-1,1',3,3'-tetraethylbenzimi-dazolylcarbocyanine-iodide), a monomeric fluorescent dye, capable of selectively entering mitochondria was used to analyze mitochondrial membrane potential. It yields green fluorescence in dead cells and red fluorescence in live cells. Cells were incubated with JC-1 (10mg/ml DMSO) (Molecular Probes, OR, USA) for 15 min at RT and subsequently acquired at 530 nm.

Immunohistochemistry

About 5 µm thick mice ovarian sections were deparaffinized in xylene and hydrated through grades of alcohol. Sections were quenched for 30 min in 0.3% (v/v) hydrogen peroxide in 100% methanol to block endogenous peroxidase and antigen retrieval was done using citrate buffer (pH 6.0). Sections were then blocked with 3% bovine serum albumin (BSA) at RT for one hour and incubated with primary rabbit polyclonal antibody to Bcl_2 and Bid (Imgenex Corporation, CA, USA) with dilutions of 1:4000 and

1:2000, respectively overnight at 4°C. Next day following a brief wash in 0.01 M PBS, sections were incubated with biotinylated goat anti-rabbit secondary antibody for an hour, followed by 30 min incubation with HRP- Streptavidin conjugate. It was visualized by detection with diaminobenzidine as a chromogen. The sections were subsequently counterstained with haematoxylin, dehydrated in xylene and mounted in dibutyl phthalate xylene (DPX) for microscopic examination. Primary antibody was omitted in negative controls and substituted with 0.01M PBS. Localization of pro- and antiapoptotic molecules, Bid and Bcl_2, respectively, were visualized under the Leica DMLA (Wetzlar, Germany) microscope. Images of 10 different fields were acquired and analyzed using Image J software (version 1.50i, NIH, USA) for each experimental group. Quantification of proteins in the cells was carried out using Image J software (version 1.50i, NIH, USA) and results, expressed as mean O.D $\pm$ SEM.

Immunofluorescence

Ovaries were collected from control and treated group mice of 12 weeks and fixed in 4% paraformaldehyde (PFA) (Sigma, MO, USA) in PBS. Immunolocalization was carried out on 5 um thick sections using 1:50 dilution of polyclonal antibody of caspase 9, (Abcam, UK) with the Alexa fluor 488 goat anti-rabbit SFX kit (Molecular probes, OR, USA). Five µm thick mice ovarian sections were deparaffinised in xylene and antigen retrieval was done using citrate buffer (pH 6.0). After permeabilisation with PBS with 0.2% Triton X100, sections were then blocked with 2% bovine serum albumin (BSA) at RT for one hour and incubated with primary rabbit polyclonal antibody. Nuclear staining was carried out with PI, which was added along with the secondary antibody. Slides were mounted with Vectashield (Vector Laboratories, Inc., CA, USA). Images were captured using LSM 510 Meta confocal system (Carl Zeiss, Jena, Germany) and quantified as described above by Image J software (version 1.50i, NIH, USA).

Electron Microscopy studies

Ovaries of 12th wk mice from each group were used for electron microscopic studies. The ovaries were fixed in modified Karnovsky's fluid[23] for 4-6 h and then rinsed twice in 0.1M sodium cacodylate buffer at 4°C. The tissues were fixed with 1% osmium tetroxide, subjected to dehydration using ascending grades of acetone and embedded in Araldite resin (Pelco International, CA, USA). Ultrathin sections (60-70 nm) were cut on UCT-R ultra-microtome (Leica, Wetzlar, Germany) and picked up on uncoated copper grids (200 mesh). These sections were stained with uranyl acetate and contrasted with lead citrate. The grids were viewed in the transmission electron microscope (TEM) Philips Tecnai G12 (Eindhoven, Netherlands) at an accelerating voltage of 80 KV and images were captured with 3.1 version of SIS software (Eindhoven, The Netherlands) supplied by the manufacturer. The nucleus to cytoplasmic ratio was measured in twelve cumulus granulosa cells, six from control and six from treated group.

Statistical analysis

Statistical analyses were carried out using unpaired Student's t-test in Graphpad Prism software (Version 6). $P < 0.05$ was considered to be statistically significant.

Results

Effect of neonatal exposure of estradiol on fecundity

The estradiol treated mice showed precocious vaginal opening between 24 and 26 days whereas control animals showed between 29 and 30 days, suggesting an early onset of puberty in treated animals. Further, animals from the treated group showed persistent vaginal cornification (PVC), and remained in constant estrus during the entire study. The control mice delivered 5-6 pups/animal but none of the treated animals became pregnant and fecundity remained nil.

Neonatal exposure of estradiol on body and ovarian weight

Body weight of the treated animals was significantly lower throughout the study (Fig. 1A). The ratio of ovary weight per 100 g body wt. showed significant increase at 4th wk, however, sharp decline was observed in treated mice beyond 16 weeks which coincided with the appearance of PVC (Fig. 1B).

Morphometric Analysis

To precisely quantify the effect of neonatal exposure of estradiol on ovarian folliculogenesis, we carried out morphometric analysis in the 12-week treated mice ovaries (Fig. 1C). There was a significant increase in the number of preantral follicles in the treated group as compared to the control group (4.93+0.4 *vs*. 1.88+1.02, P=0.049). However, the number of Graafian follicles was significantly decreased in treated group (0.92$\pm$0.03 *vs*. 2.96$\pm$0.36, P=0.005) compared to the control group, with complete absence of corpus luteum (CL).

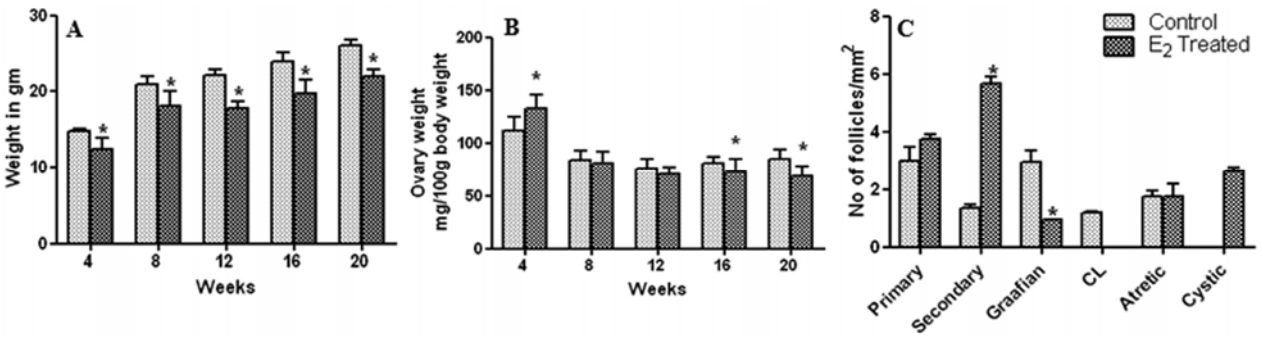

Fig. 1 — Baseline parameters of study animals. Figs. 1A and 1B depict the body weight and ovary weight relative to body weight of control and treated mice, respectively (n=15 pups/group). Fig. 1C depicts the morphometric analysis of the number of follicles per mm^2 of the ovary of control and treated mice (n=3 pups/group). [Statistically significant differences using unpaired student's t test (P <0.05) between the two groups have been marked with an asterisk]

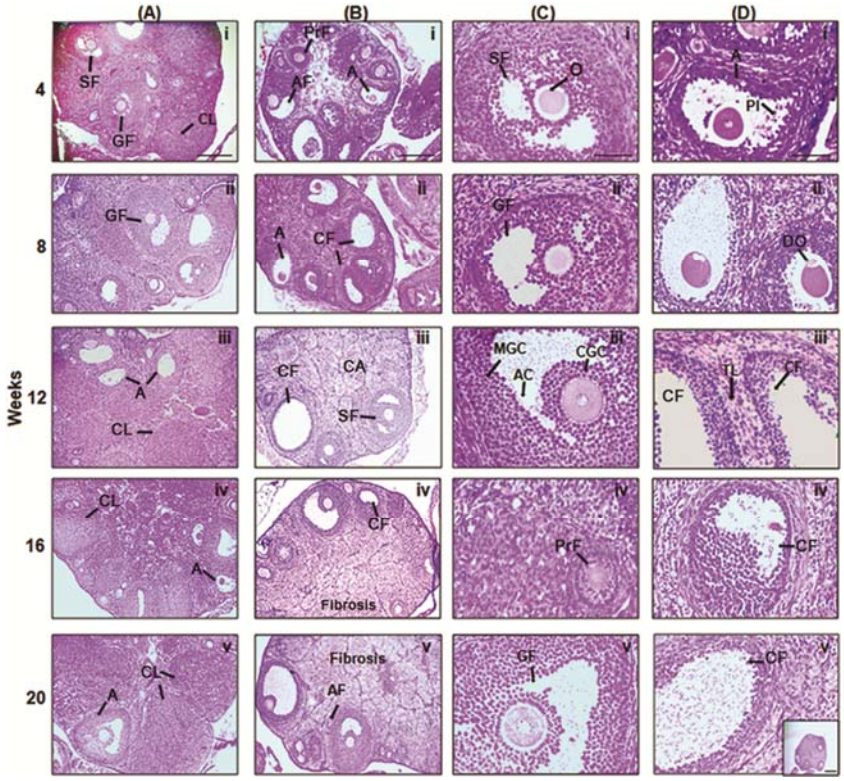

Fig. 2 — Effect of 17 β-estradiol on folliculogenesis. [Representative histological overview of Haematoxylin–Eosin stained ovaries from both control and treated mice (n=3 animals/group for each time point). Panel (A and C) represents the ovarian section showing follicles at different stages of folliculogenesis with presence of corpus luteum, obtained from control group of mice at 10 and 40X, respectively. Panel (B and D) represents cystic ovary with arrested follicles with pyknotic inclusions from 17 β-estradiol treated mice at 10 and 40X respectively. PA= Preantral Follicle; AF= antral follicle; PrF= Primordial follicle; GF= Graafian follicle; A= atretic follicle; CF=cystic follicle; CL= corpus luteum; MGC= mural granulosa cells; CGC= cumulus granulosa cells; AC= antral cavity; O= oocyte; DO= degenerating oocyte; PI= pyknotic inclusions; TL= theca layer. Row in each panel (i) 4 weeks animal, (ii) 8 weeks animal, (iii) 12 weeks animal, (iv) 16 weeks animal, and (v) 20 weeks animal. Scale bar (10X) = 500 μm; Scale bar (40X) = 50 μm

Gonadotropin level

We have not observed any significant difference in either FSH (4.59±0.36 *vs*. 3.27±1.4, *P*= 0.154) or LH (0.19±0.03 *vs*. 0.35±0.23, *P*=0.240) levels measured at 12th wk between the control (n=3) and treated (n=3) groups.

Assessment of follicular development

Presence of numerous corpora lutea along with developing follicles of various stages in control group confirms ovulation (Fig. 2 A(i)-A(v), 10X). At 4 weeks, antral follicles with detached pyknotic granulosa cells in the antrum and degenerated oocyte

(Fig. 2 D(i), 40X) were observed, indicating atresia in the treated group. Further, at 8 weeks (Fig. 2 B(ii), 10X), small cystic follicles start appearing. The antral follicles showed increased degeneration with some showing loss of cumulus granulosa cells (Fig. 2 D(ii), 40X) and others with disappearance of oocytes (Fig. 2 B(ii), 10X). After 12 weeks exposure to estradiol, the ovary showed prominent cystic follicles with large antral cavity and pyknotic inclusions which were enclosed by scanty granulosa layer with hyperplastic theca layer (Fig. 2 D(iii) 40X), and no CL suggesting anovulation. Additionally, at 16 and 20 weeks, the cystic follicles appear shrunken and cell clusters are uniformly scattered throughout the stroma, encapsulated by basement membrane (Fig. 2 D(iv) and D(v), 40X). Early luteinisation of cystic follicles is also observed with subsequent fibrosis (Fig. 2 B(iv) and B(v), 10X). Thus, it was noted that estradiol injection induces cystogenesis.

Effect of estradiol treatment on viability of granulosa cells

As pyknotic granulosa cells were observed in histological section of treated ovaries, we assessed the viability of the cells using FDA (Fig. 3A). Decrease in live cell population was observed from 8th wk onwards after treatment. Marked decrease in the percentage of viable granulosa cells in treated and control group at 12th wk (8.43±3.17 *vs.* 85.01±0.79/ P <0.05) indicated that estradiol treatment induces granulosa cell death.

DNA fragmentation of granulosa cells

DNA fragmentation is the hallmark of apoptosis which was studied using PI staining (Fig. 3 B). We observed a dramatic increase in percentage of granulosa cells at sub G_0 phase (fragmented DNA) of cell cycle in treated group indicating increased apoptosis compared to the control group (52.14±0.73 *vs.* 12.90±0.46, P <0.05) at 12th wk. This may be due to marked presence of cystogenesis in treated ovaries as atretic follicle count was comparable between the control and treated groups.

Analysis of anti- and pro-apoptotic molecules

Apoptosis in cells occurs by two main pathways: the extrinsic pathway and the intrinsic pathway. To understand the apoptotic processes associated with

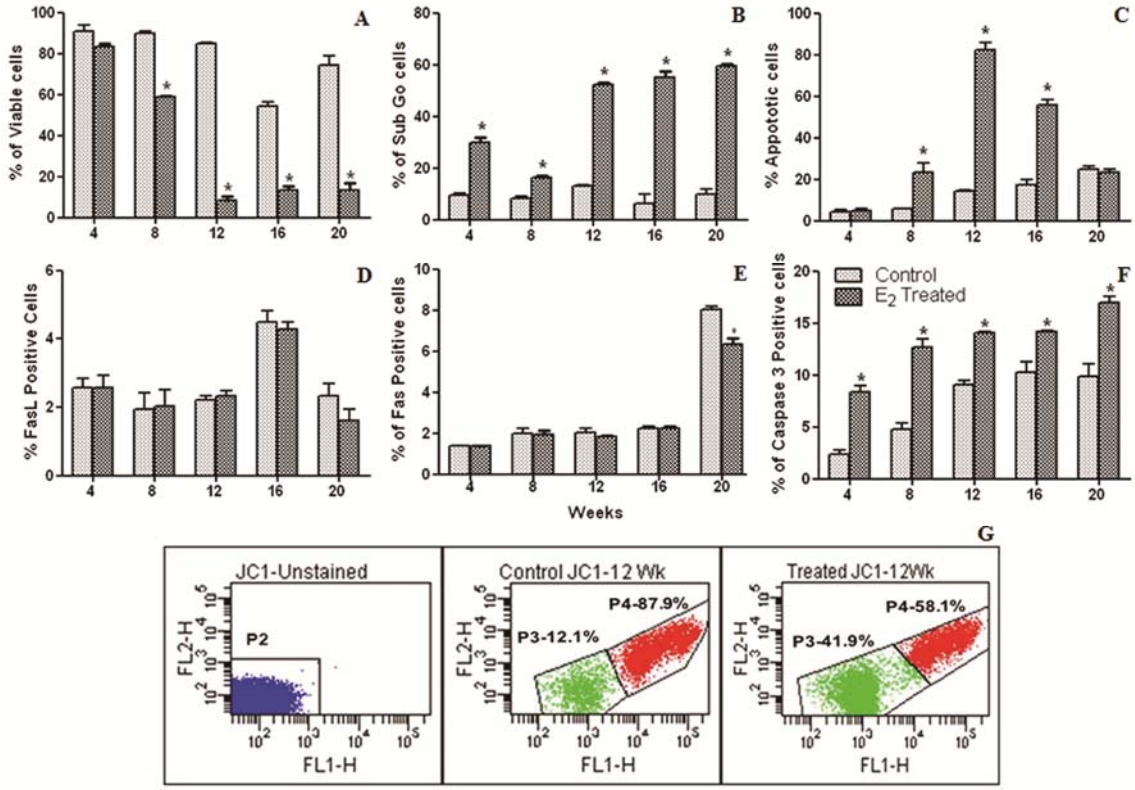

Fig. 3 — Comparative flow cytometry analyses of granulosa cell populations obtained from control and 17β estradiol treated groups, (n=3 animals/group/time point pooled) after staining with FDA (cell viability) (A); apoptotic cells by PI staining (Sub G_0 cells) (B); JC-1 (mitochondrial membrane potential) (C); FasL (D); Fas (death receptor pathway proteins); (E), and active caspase 3 (final executor) (F); and Fig. 3G is a dot-plot representing JC-1 expression in 12th week treated animals compared to control animals. [Statistically significant differences by unpaired student's t test (P <0.05) between the two groups have been marked with an asterisk]

cystogenesis, we analysed expression of different anti and pro-apoptotic markers of both pathways in granulosa cells of estradiol treated and vehicle treated mouse ovaries.

Mitochondrial membrane potential (ψm) in granulosa cells

Apoptosis induced by mitochondrial dysfunction alters its membrane potential (MMP) which can be measured by JC-1 staining. It was observed that neonatal estrogenization induces a significant increase in the population of cells with low MMP i.e., apoptotic cells, 8th wk onwards (20.32±0.15 *vs.* 5.94± 0.02, P <0.05), at 12 th wk (82.5± 3.35 *vs.* 14.53±0.59, P <0.05) till 16th wk (56.02± 2.17 *vs.* 17.55±2.07, P <0.05) as compared to control (Fig. 3C).

Expression of death receptor Fas Ligand and Fas in granulosa cells

The extrinsic pathway that initiates apoptosis involves transmembrane receptor-mediated interactions of FasL and Fas. The effects of estradiol injection on the expression of FasL/Fas in granulosa cells were studied. It was noted that there was no significant difference in the expression levels of both FasL and Fas at 4, 8, 12, and 16 weeks between both groups. However, at 20th wk we observed decrease in Fas expression in the treated mice compared to controls (Fig. 3D and 3E).

Expression of caspase 3 in estradiol treated animal

Caspase 3 is the ultimate effector caspase associated with initiation of death cascade. There was significant increase in cleaved caspase 3 population in all treated groups studied at different time points compared to the control group, confirming increase in apoptosis by estrogen treatment (Fig. 3F).

Estradiol treatment alters expression pattern of Bcl_2 and Bid

The immunohistochemical localization pattern of apoptotic molecules Bcl_2 and Bid in the control and treated ovaries during development of cystogenesis are shown in Fig. 4. Maximum apoptosis was observed at 12th wk in treated mice. Upon quantifying the staining intensity of the follicle, we observed that there was significant decrease in Bcl_2 expression (83.8+3.63 *vs.* 117.76±3.85, P=0.0004) with significant increase in Bid expression (99.39+2.09 *vs.* 75.19±3.28, P=0.0004) in granulosa cells of follicle of treated mice compared to controls. Detailed localization analysis showed expression of Bcl_2 in theca layers, granulosa cells and oocytes of control mice (Fig. 4B), and mainly in thecal cell layer of cystic follicle in treated mice (Fig. 4C). On the other hand, intense localization of Bid (Fig. 4E) was observed only in CL (Fig. 4E insert) of control animals and GCs of cystic follicles of treated mice (Fig. 4F). Together, our findings indicate that apoptosis occurs mainly via the intrinsic pathway in cystic ovarian follicles.

Expression of caspase 9 in estradiol treated animal

A significantly increased expression of caspase 9 was observed in granulosa cells of cystic follicles in the treated group compared to granulosa cells of

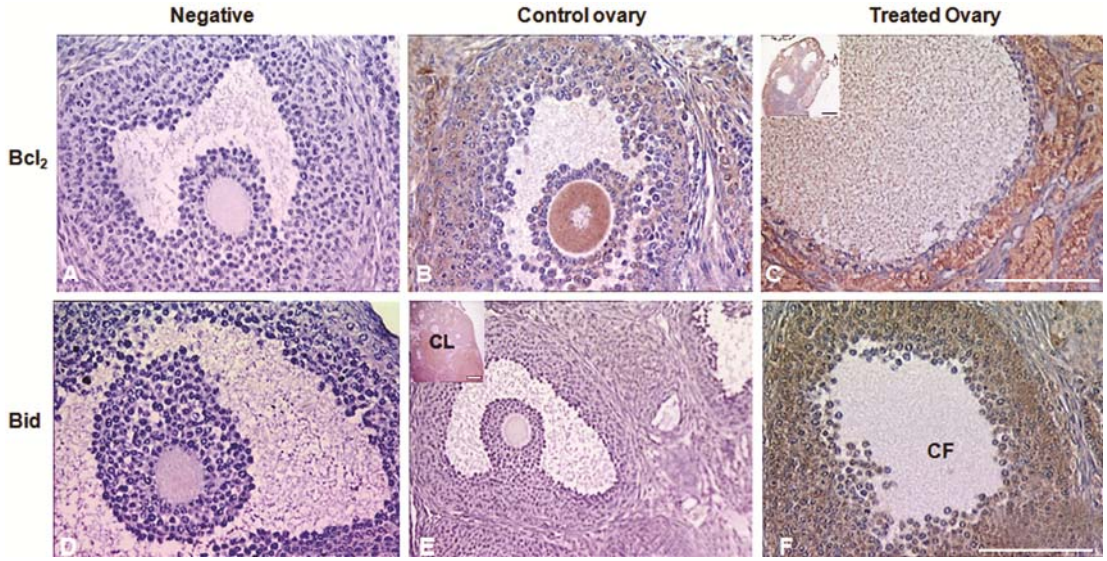

Fig. 4 — Immunohistochemical localization of anti-and pro-apoptotic markers using antibodies against Bcl_2 (A-C) and Bid (D-F) in ovaries of control and treated mice at 12th week (n=3 animals/group). [Note that the distribution of Bcl_2 was visible in all cells of control ovary but restricted to only theca cells of cystic ovary. On the other hand, Bid expression is observed in the granulosa cells of cystic follicle (CF) and only in the corpus luteum (CL, insert) of control ovary. Scale Bar = 100 μm]

control ovary (62.33±3.72 *vs*. 27.04±3.65, *P*=0.0003) (Fig. 5), which indicates activation of apoptotic pathway in cystic follicles of treated animal

Ultrastructural study of ovary in estradiol treated mice

Detailed ovarian morphology of both control and treated animals at 12 th wk were evaluated using TEM. The control group showed bilayer of thecal cells (Fig. 6A) along with normal granulosa cells (Fig. 6B). Treated ovary showed multiple thecal layers (Fig. 6D) along with degeneration of the granulosa cells marked by vacuolization and formation of apoptotic bodies (Fig. 6E). The cystic follicles have undergone fibrosis showing dense cytoplasm, pyknotic nuclei and loss of transzonal microvilli projections between oocyte and granulosa cell (Fig. 6F) which are otherwise maintained in control follicle (Fig. 6C). Cumulus granulosa cells (CGCs) of treated group show slightly decreased nucleus to cytoplasm ratio compared to control CGCs, though it was not statistically significant (0.79±0.15 *vs*. 0.89±0.28, *P*=0.49).

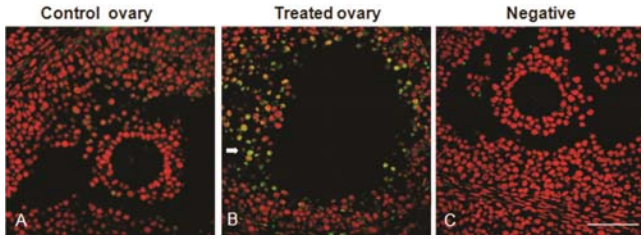

Fig. 5 — Immunofluorescent detection of caspase 9 in ovaries of control and 17β-estradiol treated mice at 12th week (n=3 animals/group). (A) and (B) represent merged image of caspase 9 (green, FITC) and counterstained (red, propidium iodide, PI) control (Graafian follicle) and treated (cystic follicle) ovaries, respectively. Corresponding negative controls are shown in panel (C). [Scale bar= 50 μm]

Discussion

The current study has revealed that neonatal estrogenization of mice has an adverse effect on ovary affecting normal folliculogenesis which is manifested by arrest in follicular growth, development of cysts and anovulation leading to infertility. The cystic follicle showed increased apoptosis and detailed analysis revealed that during cystogenesis, apoptosis is initiated predominantly via mitochondrial pathway. Several animal models have been developed by hormonal or physiological manipulations to induce key characteristic features of PCOS such as polycystic ovaries, anovulation, and metabolic disturbances for better understanding of mechanism of disrupted folliculogenesis in PCO[24]. The closest PCOS like features have been reported in female rhesus monkeys following exposure to high levels of androgen in utero[25]. However, as no model has been able to replicate PCOS completely, with inconsistent features varying according to the experimental strategy, so it has been proposed to select appropriate models to study distinct aspects of the syndrome[26]. Rodent models show evolutionarily conserved features of hypothalamic-pituitary regulation of reproduction as

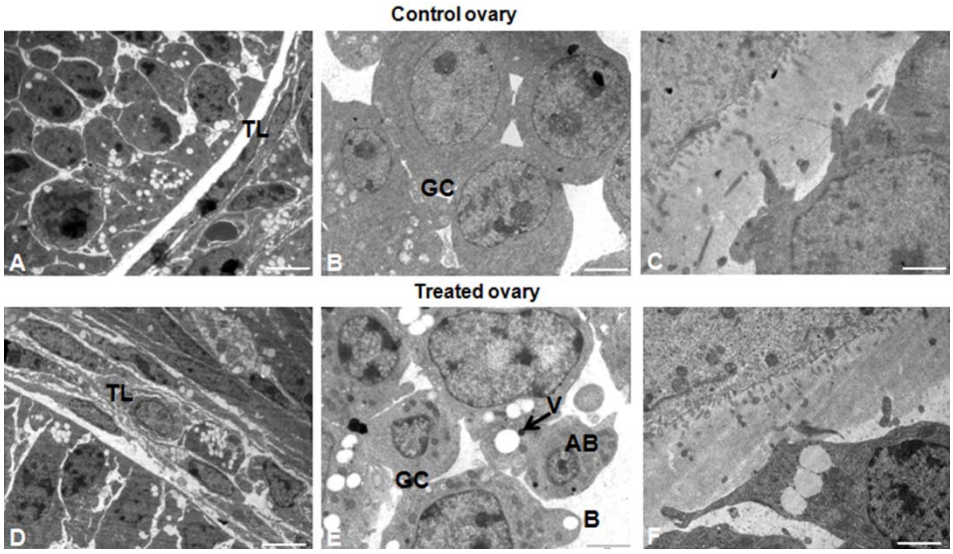

Fig. 6 — Representative ultramicrograph of section of ovary at 12th weeks (n=3 animals/group). Panels (A) and (B) show theca bilayer and normal granulosa cells (GC) in control mice respectively. Panels (D) and (E) show cystic follicle with multi layered theca cells and granulosa cells (GC) with characteristic apoptotic features including intense vacuolization (V), blebbing (B) and formation of apoptotic bodies (AB) in 17β-estradiol treated mice. Panels (C) and (F) show oocyte-granulosa cell interactions in the follicles of control and treated mice, respectively. [Scale bar (A and D) = 5 μm; Scale bar (B, C, E and F) = 2 μm]

well as folliculogenesis similar to humans and hence are advantageous in developing models to observe as well as investigate the underlying molecular mechanism of development of morphologic features of PCOS[25]. The neonatally estrogenized mouse model developed in our lab shows typical features of cystic ovary, which is a chief morphological attribute characteristic of PCOS.

Naturally occurring or synthetic compounds identified as endocrine disruptors modify the effects of steroid hormones[27]. It has been suggested that an animal model like ours can help towards determining the risk of early exposure to steroids or steroid mimicking compounds and possible abnormal programming which may occur in response to these compounds leading to metabolic and reproductive dysfunction[24]. Earlier studies have shown that neonatal or prenatal estrogen administration in rodent models permanently damage the female reproductive system resulting in lack of ovulation, decreased serum levels of gonadotropins and estradiol, and development of cystic follicles in adulthood[18,19]. Many estrogen mimicking compounds disturb pituitary gonadal axis, ovarian folliculogenesis, ovulation and implantation[27]. Our murine model of cystic ovary has been developed in Swiss mice by a single injection of 17β-estradiol during a specific window of postnatal period i.e. on postnatal day 5 similar to earlier reports,[18,19,28] which have clearly shown that treatment with steroids in the neonatal stage i.e. first week of life disturbs gonadal development in adulthood. Characterization of our mouse model has shown that an increased number of follicles start developing but get arrested at the preantral stage, with consequent development of cystic follicles with thickening of thecal layer and reduction in granulosa cell layers and complete absence of CL indicating anovulation. Interestingly, estradiol treatment induced a decrease in the ovarian weight, despite increased proliferation of theca interna cells and large fluid filled antral follicles in ovary. These mice remained in constant estrus with subsequent anovulation and infertility. In line with these observations, rats treated neonatally with estradiol valerate presented with precocious vaginal openings, disrupted cyclicity and anovulation, decrease in antral follicles and increased number of cystic follicles and absence of CL[15-17]. We report that neonatal estrogenization induced increased luteinisation of granulosa cells, shrinkage and gradual loss of oocyte and fibrosis of the follicle. These results are in agreement with an earlier study wherein androstenedione treated mice show enhanced apoptosis in the inner granulosa cell layers, with oocyte removal and spontaneous luteinisation[29]. Thus, collectively, ovarian histology of treated animals in our study shows the presence of large cystic follicles devoid of oocytes, with complete absence of CL, enlarged ovarian stroma with greater volume of theca interstitial cells, thereby confirming arrest in follicular growth and maturation.

In addition to morphological features, we have observed that both LH and FSH were comparable between the control and treated groups at the 12th wk. A major limitation is that we have not measured estradiol and testosterone levels in the present study. However, in a similar mouse model Deshpande *et al.*[18]. report low circulating levels of serum estradiol, which may contribute to the lack of preovulatory surge of gonadotropins leading to anovulation in mice.

Our study has tried to delineate the apoptotic changes in the ovary at different time points of post estrogenization which to the best of our knowledge has not been previously reported. We demonstrated a significantly progressive decrease in the number of viable cells in the ovarian follicles of the treated group compared to control, which may be due to the degradation and dispersion of the follicular cells, beginning at 8 weeks. Further, increased DNA fragmentation observed in granulosa cells of treated mice supports presence of apoptosis in the cystic follicles, similar to that seen in light exposed rat model of cystic ovaries[12,30]. An increase in the apoptotic cells following androgenization has also been previously demonstrated in rat cystic follicles[12,29,31]. Although we have observed progressive increase in the number of apoptotic cells from the 4th wk of treatment onwards, the 12th wk follicle provides the strongest morphological changes and was chosen for subsequent assays.

Ultrastructure studies of 12 th wk treated ovary highlights prominent cystic follicle with occurrence of apoptotic bodies along with large cytoplasmic vacuoles in granulosa cells, similar to those found in a DHEAS induced PCO model[31]. On the other hand, the control mice followed the normal pattern of degenerative follicular atresia. The trend towards decrease in nucleus to cytoplasm ratio in CGCs of treated animals may be due to increase in cytoplasmic content associated with cytoplasmic vacuolization and

blebbing in conjunction with nuclear shrinkage. Oocyte-granulosa cell crosstalk is essential for follicular growth and survival. We have observed loss in oocyte-granulosa cell transzonal projections which may affect communication between them, thus contributing towards cell death with subsequent loss of both oocyte and granulosa cells.

Apoptosis is triggered mainly through two pathways; the death receptor pathway and the mitochondrial pathway[32]. Death receptor pathway is activated by binding of Fas, tumor necrosis factor (TNF), and TRAIL ligands to their death receptors on cell surface and activates caspase 8 which initiate apoptosis. The mitochondrial pathway involves pro- and antiapoptotic members of the Bcl_2 family, and the imbalance between these molecules affects mitochondrial membrane potential, leads to release of apoptogenic proteins into cytoplasm and triggers the execution of cell death by promoting caspase 9 activation[33]. Several other molecules are involved in crosstalk between these two diverse pathways. Eventually activation of the final executor, caspase 3 occurs, resulting in DNA fragmentation, cleavage of key cellular proteins leading to cell death. Earlier reports from our lab showed follicular atresia occurring during normal folliculogenesis is mediated through Fas-FasL receptor pathway[34,35]. However, as the precise apoptotic mechanism during cystogenesis still remains unclear, we measured apoptotic markers representing both the extrinsic and intrinsic apoptotic pathways over 20 weeks post estrogen administration. We found that a large number of cells displayed low mitochondrial membrane potential in the treated group suggesting activation of mitochondrial pathway of apoptosis from 8th wk of treatment onwards.

The activation of apoptotic process in the mitochondria depends on the balance between anti- (Bcl_2 and Bcl-XL) and pro-apoptotic (Bad, Bax or Bid) members of the Bcl_2 family of proteins[36]. We have observed low expression of antiapoptotic Bcl_2 and increased expression of pro-apoptotic Bid in cells of cystic follicle at 12 weeks supporting activation of mitochondrial pathway leading to disruption of mitochondrial membrane potential. We also observed significantly intense expression of caspase 9 in granulosa cells of cystic follicles at 12th week, supporting yet again involvement of mitochondrial pathway during cystogenesis. The expression of FasL and Fas showed no significant difference between control and treated animals between 4-16 weeks. However, Fas expression in treated animals was significantly decreased compared to control animals at 20 th wk. This suggests that the Fas/FasL death receptor pathway may not be involved in apoptotic process induced by estrogen treatment in mice ovary.

The death receptor and mitochondrial pathway of apoptosis converge on the same executor pathway which is initiated by activation of caspase 3[37]. During the progression of cystogenesis, we see a significant increase in the percentage of active caspase 3 positive granulosa cells in the estrogen treated group compared to controls, beginning at the 4 th wk itself. Light induced rat model of cystic ovary also showed increased caspase 3 expression in granulosa cells[38]. In contrast, low proliferation coupled with low expression of caspase-3 have been implicated towards slow growth and maintenance of cystic follicles in Holstein-Friesian cows[11]. Further, human follicles derived from anovulatory PCOS women show decreased apoptotic rates as substantiated by decreased levels of caspase 3[39]. However, it is important to note that the follicles in cow and human studies are fully developed follicular cysts which remain static and persist for long time, and therefore, may show decreased caspase 3 expressions. To our knowledge, this is the first report which shows that mitochondrial pathway of apoptosis is highly activated in cells of cystic follicles resulting in senescence subsequent to estrogen administration in neonatal mice. However, this model needs to be characterized further.

Conclusion

The current study clearly emphasizes that this neonatally administered estrogen dose was sufficient to satisfactorily demonstrate unfavourable effects on the ovarian morphology including follicular growth arrest, premature luteinisation, formation of prominent follicular cysts, coupled with anovulation, cessation of cyclicity and early senescence of follicles. Our findings indicate that neonatally estrogenized mice parallel PCOS like features in the human ovary. We have also established that there is an increase in apoptosis, and particularly the mitochondrial pathway is enhanced in cystic follicles. Further, we have recorded time dependent changes in the apoptotic pathway molecules to gain insight into the advancement of apoptosis during cystogenesis. Reports on fertility impairing estrogenic endocrine disruptors have received more attention, but in depth

investigations are required to understand the mechanisms of ovarian dysfunction and formulate treatment and management strategies to improve reproductive function.

Acknowledgement

This work was supported by grants from Board of Research in Nuclear Sciences (Project No. 2008/37/25/25/BRNS/2373), ICMR-National Institute for Research in Reproductive Health (RA/370/05-2016), Mumbai, New Delhi, India. The authors wish to acknowledge Ms. Reshma Gaonkar and Ms. Shobha Sonawane for their assistance in confocal microscopy, Mr. Pravin Salunkhe for obtaining sections of the ovary and Mr Pradip More for assistance in animal handling.

References

1 Goodarzi MO, Dumesic DA, Chazenbalk G & Azziz R, Polycystic ovary syndrome: etiology, pathogenesis and diagnosis. *Nat Rev Endocrinol*, 7 (2011) 219.

2 Legro RS, Arslanian SA, Ehrmann DA, Hoeger KM, Murad MH, Pasquali R & Welt CK, Diagnosis and treatment of polycystic ovary syndrome: an Endocrine Society clinical practice guideline. *J Clin Endocrinol Metab*, 98 (2013) 4565.

3 Franks S, Stark J & Hardy K, Follicle dynamics and anovulation in polycystic ovary syndrome. *Hum Reprod Update*, 14 (2008) 367.

4 Tsafriri A & Braw RH, Experimental approaches to atresia in mammals. *Oxf Rev Reprod Biol*, 6 (1984) 226.

5 Hirshfield AN, Development of follicles in the mammalian ovary. *Int Rev Cytol*, 124 (1991) 43.

6 Salha O, Abusheikha N & Sharma V, Dynamics of human follicular growth and *in-vitro* oocyte maturation. *Hum Reprod Update*, 4 (1998) 816.

7 Hughes FM, Jr. & Gorospe WC, Biochemical identification of apoptosis (programmed cell death) in granulosa cells: evidence for a potential mechanism underlying follicular atresia. *Endocrinology*, 129 (1991) 2415.

8 Tilly JL, Kowalski KI, Johnson AL & Hsueh AJ, Involvement of apoptosis in ovarian follicular atresia and postovulatory regression. *Endocrinology*, 129 (1991) 2799.

9 Nandedkar TD, Parkar SG, Iyer KS, Mahale SD, Moodbidri SB, Mukhopadhyaya RR & Joshi DS, Regulation of follicular maturation by human ovarian follicular fluid peptide. *J Reprod Fertil Suppl*, 50 (1996) 95.

10 Elmore S, Apoptosis: a review of programmed cell death. *Toxicol Pathol*, 35 (2007) 495.

11 Isobe N & Yoshimura Y, Deficient proliferation and apoptosis in the granulosa and theca interna cells of the bovine cystic follicle. *J Reprod Dev*, 53 (2007) 1119.

12 Beloosesky R, Gold R, Almog B, Sasson R, Dantes A, Land-Bracha A, Hirsh L, Itskovitz-Eldor J, Lessing JB, Homburg R & Amsterdam A, Induction of polycystic ovary by testosterone in immature female rats: Modulation of apoptosis and attenuation of glucose/insulin ratio. *Int J Mol Med*, 14 (2004) 207.

13 Honnma H, Endo T, Henmi H, Nagasawa K, Baba T, Yamazaki K, Kitajima Y, Hayashi T, Manase K & Saito T, Altered expression of Fas/Fas ligand/caspase 8 and membrane type 1-matrix metalloproteinase in atretic follicles within dehydroepiandrosterone-induced polycystic ovaries in rats. *Apoptosis*, 11 (2006) 1525.

14 Kandaraki E, Chatzigeorgiou A, Livadas S, Palioura E, Economou F, Koutsilieris M, Palimeri S, Panidis D & Diamanti-Kandarakis E, Endocrine disruptors and polycystic ovary syndrome (PCOS): elevated serum levels of bisphenol A in women with PCOS. *J Clin Endocrinol Metab*, 96 (2011) E480.

15 Cruz G, Barra R, Gonzalez D, Sotomayor-Zarate R & Lara HE, Temporal window in which exposure to estradiol permanently modifies ovarian function causing polycystic ovary morphology in rats. *Fertil Steril*, 98 (2012) 1283.

16 Sotomayor-Zarate R, Tiszavari M, Cruz G & Lara HE, Neonatal exposure to single doses of estradiol or testosterone programs ovarian follicular development-modified hypothalamic neurotransmitters and causes polycystic ovary during adulthood in the rat. *Fertil Steril*, 96 (2011) 1490.

17 Sotomayor-Zarate R, Dorfman M, Paredes A & Lara HE, Neonatal exposure to estradiol valerate programs ovarian sympathetic innervation and follicular development in the adult rat. *Biol Reprod*, 78 (2008) 673.

18 Deshpande RR, Chang MY, Chapman JC & Michael SD & Alteration of cytokine production in follicular cystic ovaries induced in mice by neonatal estradiol injection. *Am J Reprod Immunol*, 44 (2000) 80.

19 Pinilla L, Trimino E, Garnelo P, Bellido C, Aguilar R, Gaytan F & Aguilar E, Changes in pituitary secretion during the early postnatal period and anovulatory syndrome induced by neonatal oestrogen or androgen in rats. *J Reprod Fertil*, 97 (1993) 13.

20 Fernandez M, Bourguignon N, Lux-Lantos V & Libertun C, Neonatal exposure to bisphenol a and reproductive and endocrine alterations resembling the polycystic ovarian syndrome in adult rats. *Environ Health Perspect*, 118 (2010) 1217.

21 Rosa ESA, Guimaraes MA, Padmanabhan V & Lara HE, Prepubertal administration of estradiol valerate disrupts cyclicity and leads to cystic ovarian morphology during adult life in the rat: role of sympathetic innervation. *Endocrinology*, 144 (2003) 4289.

22 Choudhury A & Khole VV, HSP90 antibodies: a detrimental factor responsible for ovarian dysfunction. *Am J Reprod Immunol*, 70 (2013) 372.

23 Karnovsky MJ, A formaldehyde-glutaraldehyde fixative of high osmolarity for use in electron microscopy. *Journal of Cell Biology* 27 (1965) 137.

24 Padmanabhan V & Veiga-Lopez A, Animal models of the polycystic ovary syndrome phenotype. *Steroids*, 78 (2013) 734.

25 Abbott DH, Nicol LE, Levine JE, Xu N, Goodarzi MO & Dumesic DA, Nonhuman primate models of polycystic ovary syndrome. *Mol Cell Endocrinol*, 373 (2013) 21.

26 Walters KA, Allan CM & Handelsman DJ, Rodent models for human polycystic ovary syndrome. *Biol Reprod*, 86 (2012) 149, 141.

27 Crain DA, Janssen SJ, Edwards TM, Heindel J, Ho SM, Hunt P, Iguchi T, Juul A, McLachlan JA, Schwartz J,

Skakkebaek N, Soto AM, Swan S, Walker C, Woodruff TK, Woodruff TJ, Giudice LC & Guillette LJ Jr, Female reproductive disorders: the roles of endocrine-disrupting compounds and developmental timing. *Fertil Steril*, 90 (2008) 911.

28 Barraclough CA & Gorski RA, Evidence that the hypothalamus is responsible for androgen-induced sterility in the female rat. *Endocrinology*, 68 (1961) 68.

29 Okutsu Y, Itoh MT, Takahashi N & Ishizuka B, Exogenous androstenedione induces formation of follicular cysts and premature luteinization of granulosa cells in the ovary. *Fertil Steril*, 93 (2010) 927.

30 Salvetti NR, Panzani CG, Gimeno EJ, Neme LG, Alfaro NS & Ortega HH, An imbalance between apoptosis and proliferation contributes to follicular persistence in polycystic ovaries in rats. *Reprod Biol Endocrinol*, 7 (2009) 68.

31 Anderson E & Lee GY, The polycystic ovarian (PCO) condition: apoptosis and epithelialization of the ovarian antral follicles are aspects of cystogenesis in the dehydroepiandrosterone (DHEA)-treated rat model. *Tissue Cell*, 29 (1997) 171.

32 Hengartner MO, The biochemistry of apoptosis. *Nature*, 407 (2000) 770.

33 Do Y, Ryu S, Nagarkatti M & Nagarkatti PS, Role of death receptor pathway in estradiol-induced T-cell apoptosis *in vivo*. *Toxicol Sci*, 70 (2002) 63.

34 Nandedkar TD & Balchandran PK, PMSG-induced follicular atresia in prepubertal mice. *Indian J Exp Biol*, 20 (1982) 353.

35 Dharma SJ, Kelkar RL & Nandedkar TD, Fas and Fas ligand protein and mRNA in normal and atretic mouse ovarian follicles. *Reproduction*, 126 (2003) 783.

36 Cory S & Adams JM, The Bcl2 family: regulators of the cellular life-or-death switch. *Nat Rev Cancer*, 2 (2002) 647.

37 Chitnis SS, Navlakhe RM, Shinde GC, Barve SJ, D'Souza S, Mahale SD & Nandedkar TD, Granulosa cell apoptosis induced by a novel FSH binding inhibitory peptide from human ovarian follicular fluid. *J Histochem Cytochem*, 56 (2008) 961.

38 Lombardi LA, Simoes RS, Maganhin CC, Baracat MC, Silva-Sasso GR, Florencio-Silva R, Soares JM Jr & Baracat EC, Immunohistochemical evaluation of proliferation, apoptosis and steroidogenic enzymes in the ovary of rats with polycystic ovary. *Rev Assoc Med Bras (1992)*, 60 (2014) 349.

39 Das M, Djahanbakhch O, Hacihanefioglu B, Saridogan E, Ikram M, Ghali L, Raveendran M & Storey A, Granulosa cell survival and proliferation are altered in polycystic ovary syndrome. *J Clin Endocrinol Metab*, 93 (2008) 881.